Silsesquioxanes Derived from the Bulk Polycondensation of [3-(Methacryloxy)propyl]trimethoxysilane with Concentrated Formic Acid: Evolution of Molar Mass Distributions and Fraction of Intramolecular Cycles

Patricia Eisenberg,[†] Rosa Erra-Balsells,[§] Yoko Ishikawa,[⊥] Juan C. Lucas,[†] Hiroshi Nonami,[⊥] and Roberto J. J. Williams*[,‡]

Technological Research Center for the Plastics Industry (CITIP), National Institute of Industrial Technology (INTI) and INDEMAT (University of San Martín), CC 157, 1650 San Martín, Argentina, Department of Organic Chemistry, University of Buenos Aires, Pab.2, Ciudad Universitaria, 1428 Buenos Aires, Argentina, Institute of Materials Science and Technology (INTEMA), University of Mar del Plata, CONICET, J. B. Justo 4302, 7600 Mar del Plata, Argentina, and Plant Biophysics/Biochemistry Research Laboratory, College of Agriculture, Ehime University, Matsuyama 790-8566, Japan

Received July 23, 2001; Revised Manuscript Received November 12, 2001

ABSTRACT: The polycondensation of [3-(methacryloxy)propyl]trimethoxysilane was performed in bulk, using 98 wt % formic acid (molar ratio HCOOH/Si = 3 or 6), at 50 or 70 °C, for periods of time of up to 1 month. The resulting silsesquioxanes (SSOs) were characterized by ^{1}H NMR, FTIR, SEC, UV−MALDI−TOF MS (linear, reflector, and post-source decay modes), and ESI−TOF MS. The residual concentrations of Si−OCH_3 groups, and generated CH_3OH and $HCOOCH_3$, were quantitatively monitored by ^{1}H NMR during the initial stage of the synthesis. After 2 days of reaction at 50 °C, or about 6 h at 70 °C, the resulting SSO mainly contained residual Si−OH groups with only traces of Si−OCH_3 groups, as was also confirmed by FTIR and UV−MALDI−TOF MS in the reflector mode. After this time, the polycondensation continued slowly during storage at room temperature, basically through Si−OH + Si−OH reactions. The average fraction of intramolecular cycles increased continuously during the polycondensation. An average value, $f_{av} = 0.81$, was found for species containing 6−24 Si atoms in a typical reaction product. This evidenced the presence of species with relatively closed structures. In MS/MS spectra, fragmentation of one or more ester groups attached to Si atoms was observed, following a McLafferty rearrangement. The addition of water to the initial formulation (about 3:1 H_2O/Si molar ratio) led to a slower polycondensation rate and to a decrease of the average fraction of intramolecular cycles (formation of more open structures). Therefore, the use of 98 wt % formic acid was useful to synthesize SSOs containing a higher fraction of intramolecular cycles than those resulting from conventional formulations.

Introduction

The hydrolytic condensation of trialkoxysilanes, $RSi(OR')_3$, performed in the presence of water and an acid or base as catalysts, leads to products that are generically called poly(silsesquioxanes) or silsesquioxanes (SSOs).[1] The polycondensation may also be carried out using strong carboxylic acids such as trifluoroacetic acid or formic acid, in the absence of water.[2] The carboxylic acid acts both as a reactant and a catalyst. Its concentration decreases continuously, and it may be eventually depleted from the reaction mixture.

Species present in SSOs may vary from perfect polyhedra of formula $(RSiO_{1.5})_n$ (n = even number ≥ 6), also denoted as T_n or POSS (polyhedral oligomeric SSOs), to partially hydrolyzed/condensed products of generic formula $T_n(OH)_x(OR')_y$ where $T = RSiO_{1.5-m/2n}$, and $m = x + y$. Figure 1 shows examples of SSO structures for an octamer, $T_8(OH)_m$, assuming complete hydrolysis/condensation of alkoxy groups (Si atoms are indicated by circles and Si−O−Si bonds by segments; organic groups, R, attached to every Si atom are not shown).

* Author to whom correspondence should be addressed. E-mail: williams@fi.mdp.edu.ar.
[†] CITIP and INDEMAT.
[§] University of Buenos Aires.
[⊥] Ehime University.
[‡] INTEMA.

The maximum value of m is equal to $2 + n$, representing a linear/branched chain devoid of intramolecular cycles. These cycles are formed by reaction between two substituents of the same molecule, to give Si−O−Si bonds. The maximum number of intramolecular cycles is equal to $(2 + n)/2$ (for n = even) or $[(2 + n) - 1]/2 = (1 + n)/2$ (for n = odd). Its actual number is $[(2 + n) - m]/2$. Therefore, the fraction of intramolecular cycles (f) of a generic n-mer is given by

$$f = (2 + n - m)/(2 + n) \text{ (for } n = \text{even) or}$$
$$f = (2 + n - m)/(1 + n) \text{ (for } n = \text{odd)}$$

Mass spectrometry characterization of a SSO gives a primary distribution of species characterized by the number of Si atoms in their structures (n) and a secondary distribution giving the fraction of species with different values of m (or x and y) for a constant value of n. A characteristic fraction of intramolecular cycles present in a generic n-mer may be obtained by using the value of m for the species showing the highest intensity in the cluster of species with constant n. This approach has been used by Wallace et al.[3,4] to characterize the fraction of intramolecular cycles in various polymeric SSOs. For example, they found a characteristic value of $f = 0.546$ for a SSO based on [3-(methacryloxy)propyl]trimethoxysilane (MPMS).

An important question is, how can the characteristic value of f be controlled by varying the conditions of

10.1021/ma011305g CCC: $22.00
Published on Web 01/16/2002

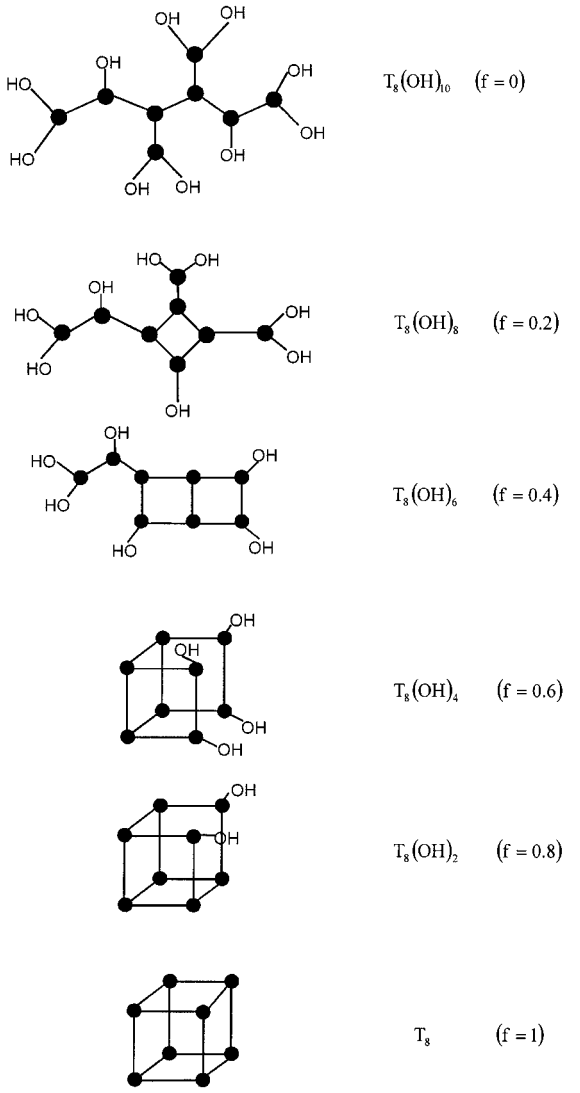

Figure 1. Examples of possible structures for an octamer of formula $T_8(OH)_m$ (circles denote Si atoms, segments represent Si−O−Si bonds, and organic groups R attached to every Si atom are not shown). *f* indicates the fraction of intramolecular cycles.

synthesis? An answer to this question will permit the synthesis of SSO with either open structures (limit of linear/branched chains, $f \rightarrow 0$) or closed structures (limit of completely condensed polyhedra, $f \rightarrow 1$) with (presumably) very different associated properties. Some trends have been recently reported regarding the influence of the type of organic group bonded to the Si atom. Wallace et al.[4] compared values of *f* for SSO with R = *n*-decyl, *n*-propyl, and 3-(methacryloxy)propyl, synthesized under similar conditions. They found that the lowest value of *f* was obtained for the [3-(methacryloxy)-propyl]SSO and suggested that H bonds between carbonyl groups and SiOH groups could be responsible for this behavior. Fasce et al.[5,6] showed that the presence of bulky organic groups favored intramolecular condensation reactions, leading to a narrow distribution of polyhedra ($f = 1$), with *n* values between 8 and 10. Matejka et al. also found that increasing the size of the organic substituent resulted in a larger fraction of intramolecular cyclization, which prevented gelation even at high conversions.[7]

The influence of the catalyst used on the synthesis on the structures of the reaction products is not well-known. A recent study reported that basic and neutral catalysts led to pronounced cyclization and self-organization of the reaction product; acid catalysts produced fewer polyhedral structures and no regular arrangements.[7] The invoked reason was a fast initial hydrolysis, leading to SiOH groups undergoing H-bond interactions with oxygen atoms in the organic chain. This led to a better compatibility, no microphase separation, and, consequently, a decrease in the fraction of intramolecular cycles (formation of more open species).

Table 1. Reaction Conditions Used for the Synthesis of Different SSOs

notation	MPMS (g)	HCOOH 98% (g)	H_2O (g)	HCOOH/Si molar ratio	H_2O/Si molar ratio	*T* (°C)	time (days)
SSO1	100	56.7	21.8	3	3.16	50	12
SSO2	100	56.7		3	0.16	50	2
SSO3	100	56.7		3	0.16	70	10
SSO4	100	113.5		6	0.31	70	9
SSO5	100	56.7		3	0.16	70	30
SSO6	100	113.5		6	0.31	70	29

The aim of this study is to analyze the effect of using 98 wt % formic acid, in the absence of extra water addition, on compositions, molar mass distributions, and average fractions of intramolecular cycles, of SSOs synthesized by the bulk polycondensation of MPMS. Some preliminary results of the evolution of molar mass distributions were previously reported.[8] Results will be compared with those obtained by adding a typical amount of extra water to the initial formulation.

Experimental Section

Synthesis of SSOs. The selected trialkoxysilane was MPMS (Dow Corning Z-6030). Its polymerization was performed in bulk with concentrated formic acid (Merck, 98 wt %), using a molar ratio of HCOOH/Si = 3 or 6. The corresponding molar ratios of water varied from H_2O/Si = 0.16 to 0.31, respectively. In one of the runs, extra water was incorporated to reach a molar ratio of H_2O/Si = 3.16. The reaction was performed in an open vessel placed in an oven at $T = 50$ or 70 °C, enabling the continuous evaporation of volatile products in circulating dry air. The polycondensation was performed for periods of time of up to 1 month.

Table 1 shows the particular reaction conditions used to synthesize the different SSOs. The reaction products were homogeneous viscous liquids that could be completely dissolved in different solvents such as tetrahydrofuran (THF) and chloroform.

Size Exclusion Chromatography. It was performed with a Shimadzu GPC 80 device, provided with a refractive index detector and using columns 801, 802, and 803, covering the range of molar masses comprised between 10^2 and 10^5 g/mol. THF was used as the carrier at a rate of 1 mL/min, and butylated hydroxytoluene (BHT), as the internal standard. Molar masses were calculated on the basis of polystyrene standards.

^{1}H NMR Spectra. Samples were dissolved in deuterated chloroform, and ^{1}H NMR spectra, recorded using a Bruker AC400 spectrometer operating at 400.13 MHz. Chemical shifts are reported as δ units (ppm) relative to tetramethylsilane.

FTIR Spectra. Infrared spectra were recorded with a Nicolet-Omnic 500 device, in the transmission mode, making coatings on KBr windows.

UV−MALDI−TOF MS. Matrix-assisted ultraviolet laser desorption/ionization time-of-flight mass spectrometry was performed using three different devices: (i) Shimadzu Kratos Kompact MALDI III, (ii) Shimadzu Kratos Kompact MALDI 4 with pulsed extraction, and (iii) PerSeptive Biosystems Voyager DE-STR. All of the devices were equipped with a pulsed nitrogen laser (λ =337 nm; pulse width = 3 ns), and

devices ii and iii were equipped with tunable PDE and post-source decay (PSD) (MS/MS device) modes.

Stainless steel probe supports (Shimadzu) were used in the Kratos Kompact MALDI III and 4 devices. Welled gold sample plates were used in the Voyager DE-STR. Samples were placed at locations which were mirror-polished.

Experiments were performed first using the full range setting for the laser firing position in order to select the optimal position for data collection and second fixing the laser firing position in the sample sweet spots. The samples were irradiated just above the threshold laser power for obtaining molecular ions and with higher laser power for studying cluster formation. Thus, the irradiation used for producing a mass spectrum was analyte-dependent. Usually 50 spectra were accumulated.

All samples were measured in linear and reflector modes, in both positive and negative ion modes. With selected matrixes and analytes, PSD experiments were also performed.

Selected matrixes were either 2,5-dihydroxybenzoic acid (gentisic acid, GA; Sigma) or *trans*-3-indoleacrylic acid (IAA; Sigma). The probe tip was coated with a solution obtained by mixing solutions of the analyte (SSO) and the selected matrix in THF (Aldrich, HPLC grade). Typically, a 10 mg/mL solution of the matrix was mixed with a 1 mg/mL solution of the analyte in an 8:1 volumetric ratio. Two coatings (0.5 μL each) were performed, removing the solvent by blowing air at room temperature after each one of them. Some runs were carried out by doping the sample with Na^+ or Ag^+. This was accomplished first by coating the probe tip with a 4.5×10^{-3} M solution of silver trifluoroacetate (AgTFA) in THF or NaCl in water and then by following with the usual procedure.

Spectra were calibrated by the use of external calibration reagents. In the linear and reflector modes, insulin, aprotinin, and α-, β-, and γ-cyclodextrin were used. In the PSD mode, the whole fragmentation patterns of angiotensin 1 and β-cyclodextrin were used, as described elsewhere.[9]

ESI−TOF MS. The positive-ion electrospray ionization time-of-flight mass spectra were acquired by directly infusing a solution of SSO in methanol−water (9:1) into the ESI ion source of the Mariner PerSeptive Biosystems ESI−TOF MS, using methanol−water (9:1) as the solvent stream. Spectra were recorded in a *m*/*z* range between 400 and 4000 Da. The spray tip potential was +3804.5 V, the nozzle potential was +250.0 V, and the skimmer voltage was +10.25 V. The nozzle temperature was 140 °C. A Harvard PHD 2000 syringe infusion pump at a flow rate of 5 μL/min was used for the introduction of the polymer solution. The nitrogen flow rate was 0.35−0.60 L/min, the analyzer temperature was kept at 29.0 °C, and the pressure was kept at 0.55 MPa. The mass calibration was achieved by using a 0.026 mg/mL solution of angiotensin 1 ($z = 1$, 1296.685 Da; $z = 2$, 648.342 Da; Sigma) in methanol−water (1:1).

Results and Discussion

Initial Stage of the Polycondensation. Possible reactions taking place during the polycondensation of tetraethoxysilane (TEOS) in the presence of concentrated formic acid have been described by Sharp.[2] For a generic $Si-OCH_3$ group of MPMS, main reactions may be written as follows:

$$Si-OCH_3 + HCOOH = Si-OOCH + CH_3OH \quad (1)$$

$$Si-OOCH + Si-OCH_3 = Si-O-Si + HCOOCH_3 \quad (2)$$

$$CH_3OH + HCOOH = HCOOCH_3 + H_2O \quad (3)$$

Besides, water initially present and generated through eq 3 participates in the usual hydrolytic condensation scheme.

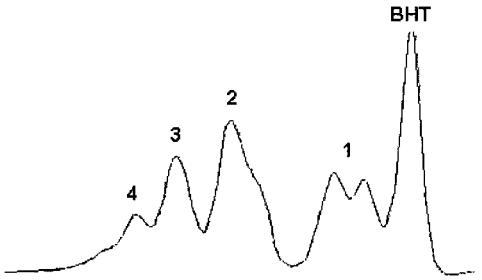

Figure 2. SEC chromatogram of the reaction product obtained after 35 min of reaction at 50 °C, during the synthesis of SSO2.

Figure 2 shows a SEC chromatogram of the products obtained after 35 min of reaction at 50 °C, during the synthesis of SSO2. The first peak at the right corresponds to the calibration standard (BHT). Main species are the monomer with different substituents, dimers, trimers, and tetramers (assignments are based on polystyrene (PS) standards).[8] After 60 min of reaction, monomers and dimers disappeared from the SEC chromatogram, giving an indication that the reactivity of any group in the condensation reaction decreases with an increase of the molar mass of the species to which it belongs. This may be ascribed to negative substitution effects produced by Si−O−Si bonds joined to the same Si atom and/or to steric effects produced by the formation of intramolecular cycles that lead to more compact structures. A similar substitution effect has been reported for the hydrolytic condensation of tetraalkoxysilanes.[10−13]

Parts a−c of Figure 3 show ^{1}H NMR spectra of the reaction products during the synthesis of SSO3 ($T = 70$ °C, HCOOH/Si = 3). The first spectrum (Figure 3a) was taken at $t = 0$, although it showed some advance in the polycondensation reaction. Peaks of the 3-(methacryloxy)propyl residue were present at 0.70 ppm (CH_2 in the position α to the Si atom), 1.75 ppm (CH_2 in the position β to the Si atom), 1.88 ppm (CH_3 group), 4.08 ppm (CH_2 in the position γ to the Si atom), and 5.51 and 6.05 ppm ($C{=}CH_2$ group). $Si-OCH_3$ protons were present at 3.52 and 3.58 ppm (multiple peaks were the result of substitution effects of neighboring groups). Protons of formic acid were evidenced at 7.99 ppm (*H*COOH) and 10.00 ppm (HCOO*H*). Methanol (CH_3-OH peak at 3.42 ppm) and methyl formate (*H*$COOCH_3$ peak at 8.02 ppm, clearly evidenced in an amplified scale, and $HCOOCH_3$ peak at 3.70 ppm) were present in the spectrum, showing the fast rate at which polycondensation occurred under the selected reaction conditions. The signal of *H*COO−Si groups could not be precise (it can be tentatively assigned to the peak present at 8.07 ppm). The peak at 7.28 ppm corresponds to the proton of undeuterated chloroform.

After 1 h of reaction (Figure 3b), peaks of CH_2 groups in the α, β, and γ positions with respect to the Si atom were broader, indicating that their mobility was constrained by the fact that a fraction of Si atoms was incorporated to cagelike structures. Significant concentrations of methyl formate (peaks at 8.03 and 3.71 ppm) and methanol (peak at 3.42 ppm) were present in the spectrum. The amount of residual $Si-OCH_3$ groups, at 3.50−3.55 ppm, showed a significant decrease. The peak of formic acid, initially present at 10.00 ppm, appeared at 6.79 ppm (the continuous shift from 10 to 6.79 ppm was monitored from spectra taken at intermediate times). The peak at 8.07 ppm was no longer present (no

direct evidence of the presence of Si−OOCH groups could be obtained, a fact that is probably related to the fast rate of their reaction with Si−OCH_3 groups).[4]

After 3 h of reaction (Figure 3c), a significant increase in the relative intensity of peaks of the 3-(methacryloxy)propyl residue was observed, giving an indication of the partial evaporation of volatile products. A very low residual fraction of Si−OCH_3 groups (peak at 3.49 ppm) remained in the reaction product, while methanol (peak at 3.38 ppm) and methyl formate (peaks at 8.02 and 3.70 ppm) were still present. The peak assigned to the hydroxyl group of residual formic acid appeared at 5.71 ppm.

After 6 h of reaction, only protons of the 3-(methacryloxy)propyl groups appeared in significant concentrations. A very small peak at 2.07 ppm, assigned to SiOH protons, also appeared in the spectrum, together with traces of methyl formate and formic acid. This constitutes the end of the initial stage of the polycondensation process. After this period, the reaction could only progress by SiOH + SiOH condensation reactions.

Protons of the 3-(methacryloxy)propyl residue kept the same relative intensities during the whole synthesis and could be used as internal standards to monitor the evolution of CH_3O groups present in different species. Taking 1 mol of the 3-(methacryloxy)propyl residue as a basis leads to 9 protons initially present in the Si−OCH_3 groups. The evolution of these groups was quantitatively followed during the syntheses at 50 °C (SSO2) and 70 °C (SSO3).

Figure 4 shows the evolution of the concentration of CH_3O− protons pertaining to Si(OCH_3) groups, CH_3OH and $HCOOCH_3$, during the first 5 h of reaction at 50 °C (synthesis of SSO2). At $t = 0$, an advance in the reaction was recorded. The amount of Si−OCH_3 protons was reduced from the initial value of 9 to about 7.1; there was 1 proton supplied by the methyl group of CH_3OH and about 0.2 protons pertaining to the methyl group of $HCOOCH_3$ (the sum gives 8.3 protons; the difference with the theoretical value may be ascribed to experimental error). The appearance of CH_3OH from $t = 0$ may be assigned to the rapid occurrence of the reaction described by eq 1 (the fraction of initially hydrolyzed Si−OCH_3 groups was 21%; the initial water present in the formulation could only account for the hydrolysis of 5% of these groups). As reactions described by eqs 2 and 3 took place, an increase in the ester concentration, together with a continuous decrease of Si−OCH_3 protons, was produced. At about 5 h of reaction, there remained 2.6 protons of Si−OCH_3 groups, together with 1.9 protons of the CH_3 group of CH_3OH and 3.7 protons of the corresponding group in methyl formate. The total number of protons was 8.2, practically the same as that initially recorded. This means that the vapor pressure of the alcohol and the ester, at 50 °C, in the corresponding solution was necessarily low enough to prevent their fast volatilization (bp = 34 °C for *pure* $HCOOCH_3$).

However, after the synthesis of SSO2 (48 h) was completed, no residual methyl protons were detected. This means that the initial Si−(OCH_3) groups were quantitatively converted into methyl formate, which was finally evaporated from the solution.

During the synthesis at 70 °C, the vaporization of methyl formate proceeded at a much faster rate. Figure 5 shows the evolution of the concentration of methyl protons pertaining to Si(OCH_3) groups, CH_3OH and $HCOOCH_3$, during the first 4 h of synthesis of SSO3. Now the total number of protons recorded at 30 min of reaction was 6.2 (theoretical value equal to 9), meaning that $HCOOCH_3$ was partially evaporated from the solution. The initial rate at which methyl formate was produced was higher than its evaporation rate, as revealed by a maximum in its concentration at about 1 h of reaction. At longer times the concentration of every species containing OCH_3 groups decreased at a fast rate. After 6 h of reaction at 70 °C, only traces of these groups remained in ^{1}H NMR spectra.

Figure 6 shows SEC chromatograms of the reaction products obtained after 4 and 6 h at 70 °C (about the end of the first stage). A bimodal distribution of molar masses was evidenced, with maxima at about $n = 6-7$ for the first peak and $n = 16-17$ for the second peak, based on PS standards. Peaks of monomers up to tetramers, which could be followed in the course of the synthesis, were absent at the end of the first stage.

^{1}H NMR and FTIR Characterization of SSOs at Advanced Degrees of Condensation. The six SSOs shown in Table 1 represent reaction products advanced to different degrees of condensation during the second stage. SSO2, SSO3, and SSO5 constitute a sequence of increasing degrees of polycondensation for the same initial formulation. SSO4 and SSO6 represent another set of such sequences.

For every product shown in Table 1, protons of the 3-(methacryloxy)propyl residue were found in the same ratio of relative intensities as that in the starting monomer. This evidenced the absence of hydrolysis of ester groups under the employed conditions (the hydrolysis would produce methacrylic acid that could be evaporated from the solution changing the relative intensity of protons in the ^{1}H NMR spectra; should it remain in solution, peaks of the acid and primary alcohol generated in the hydrolysis would appear in the spectra). Only an additional small peak present in the 2.05−2.25 ppm region, and assigned to free SiOH groups,[14−16] was found in the ^{1}H NMR spectra. Peaks corresponding to SiOH groups H-bonded between themselves, reported at 4.44 ppm, in the range 6−7 ppm, and at 7.22 ppm,[14,15,17] could not be found.

A qualitative indication of the increase in the average degree of polymerization of the SSOs was obtained by examination of the bands at about 1120 and 1040 cm^{-1} in FTIR spectra, derived from Si−O−Si antisymmetric stretches.[4] In both SSO5 and SSO6 (the most advanced products), both bands appeared in the spectra at 1128 and 1039 cm^{-1} (the former being more intense than the latter). For the less advanced SSOs, the more intense band showed a maximum at 1109 cm^{-1} and the less intense band appeared as a shoulder at 1043 cm^{-1}.

FTIR spectra also confirmed the disappearance of the O−CH_3 band present in the trialkoxysilane at 2481 cm^{-1} and the presence of SiOH groups (broad band with a maximum at 3482 cm^{-1}, assigned to stretching of OH of Si−OH groups that are hydrogen-bonded plausibly to C═O groups of methacrylates).

Both ^{1}H NMR and FTIR results clearly indicated the absence of residual Si(OCH_3) groups within the experimental error of each one of the techniques. Both techniques also detected the presence of SiOH groups that may be considered as the residual reactive positions through which the polycondensation continued at a slow rate. Traces of Si(OCH_3) groups were, however, found in UV−MALDI−TOF and ESI−TOF mass spectra to be

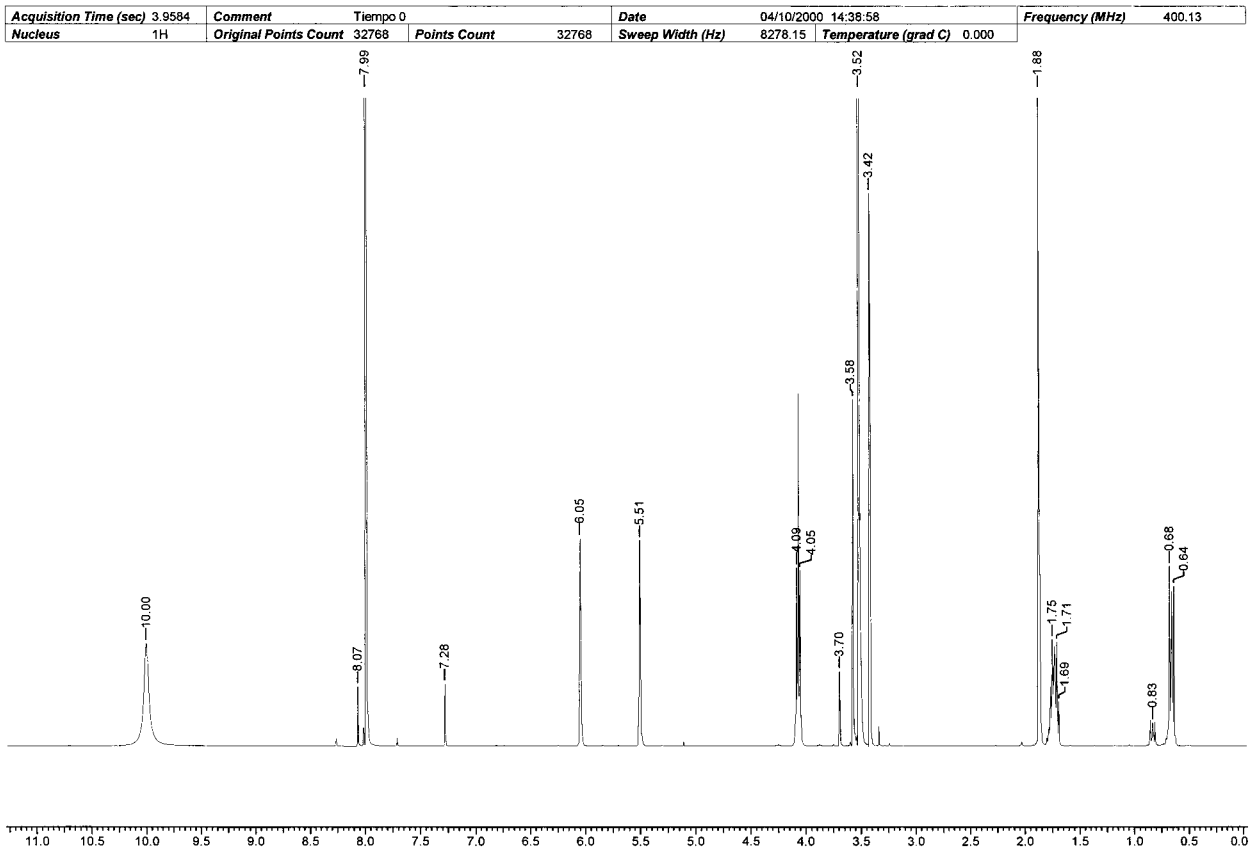
Acquisition Time (sec) 3.9584
Comment Tiempo 0
Date 04/10/2000 14:38:58
Frequency (MHz) 400.13
Nucleus 1H
Original Points Count 32768
Points Count 32768
Sweep Width (Hz) 8278.15
Temperature (grad C) 0.000
7.99
3.52
1.88
3.42
3.58
6.05
5.51
4.09
4.05
0.68
0.64
10.00
8.07
7.28
3.70
1.75
1.71
1.69
0.83
11.0 10.5 10.0 9.5 9.0 8.5 8.0 7.5 7.0 6.5 6.0 5.5 5.0 4.5 4.0 3.5 3.0 2.5 2.0 1.5 1.0 0.5 0.0

(a) t = 0

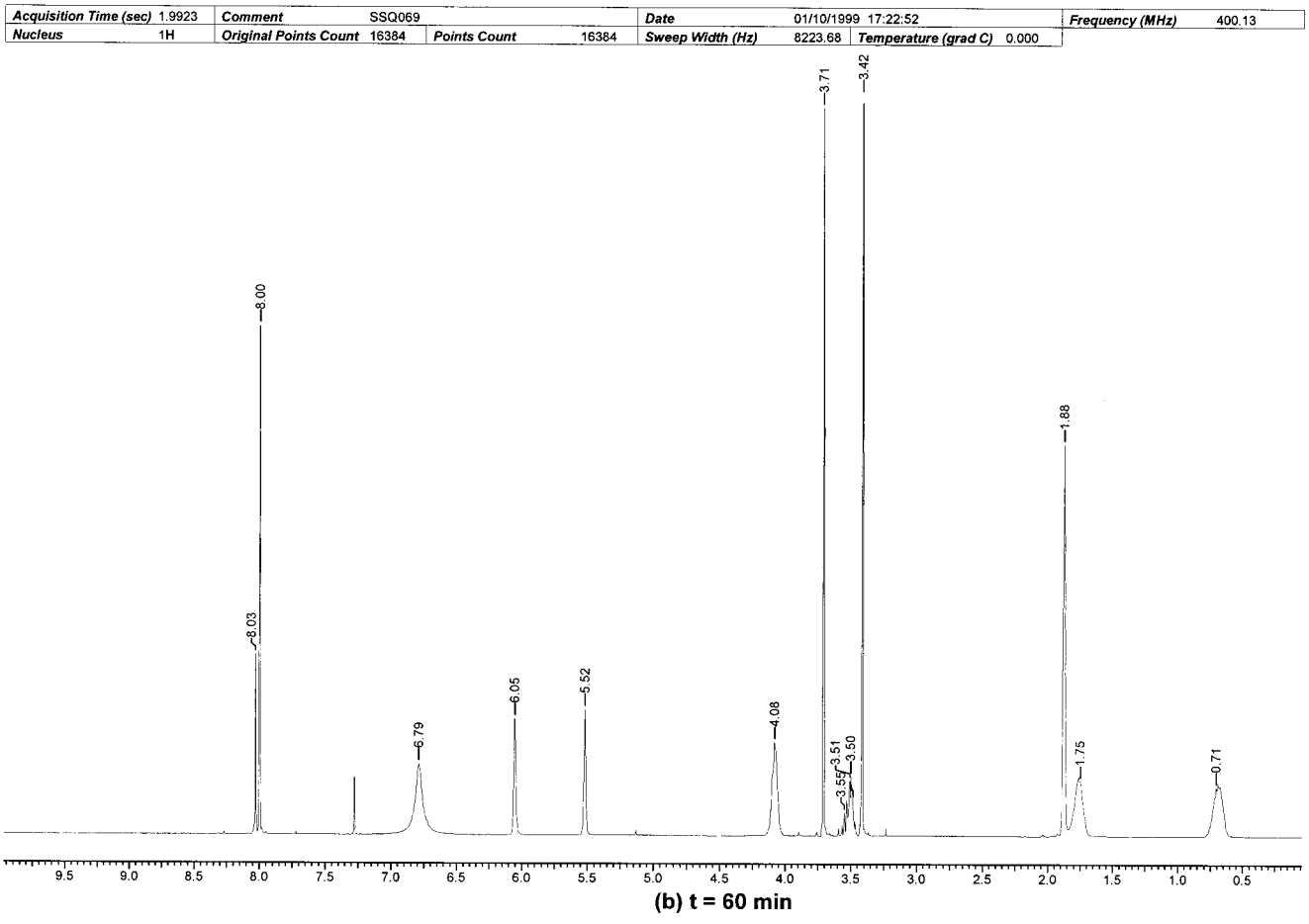
Acquisition Time (sec) 1.9923
Comment SSQ069
Date 01/10/1999 17:22:52
Frequency (MHz) 400.13
Nucleus 1H
Original Points Count 16384
Points Count 16384
Sweep Width (Hz) 8223.68
Temperature (grad C) 0.000
3.71
3.42
8.00
1.88
8.03
6.79
6.05
5.52
4.08
3.51
3.50
1.75
0.71
9.5 9.0 8.5 8.0 7.5 7.0 6.5 6.0 5.5 5.0 4.5 4.0 3.5 3.0 2.5 2.0 1.5 1.0 0.5

(b) t = 60 min

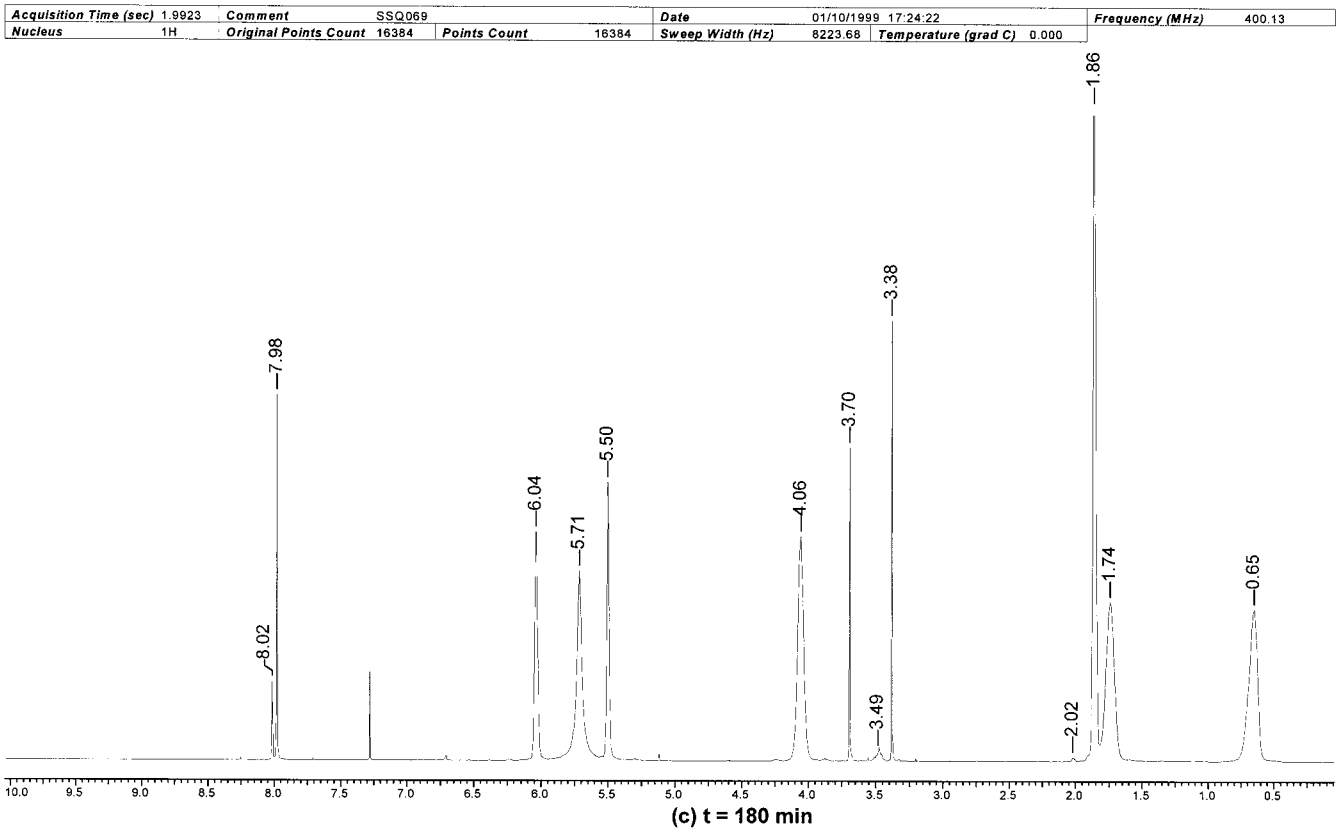

Figure 3. ^{1}H NMR spectra of reaction products during the initial stage of the synthesis of SSO3 (T = 70 °C, HCOOH/Si = 3): (a) t = 0; (b) t = 60 min; (c) t = 180 min.

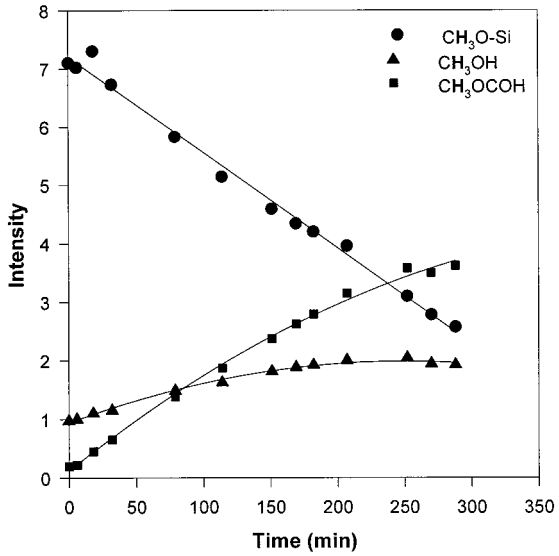

Figure 4. Evolution of the concentration of CH_3 protons pertaining to $Si(OCH_3)$ groups, CH_3OH and $HCOOCH_3$, during the first 5 h of reaction at 50 °C (synthesis of SSO2). The intensity gives the number of protons per 1 mol of 3-(methacryloxy)propyl groups.

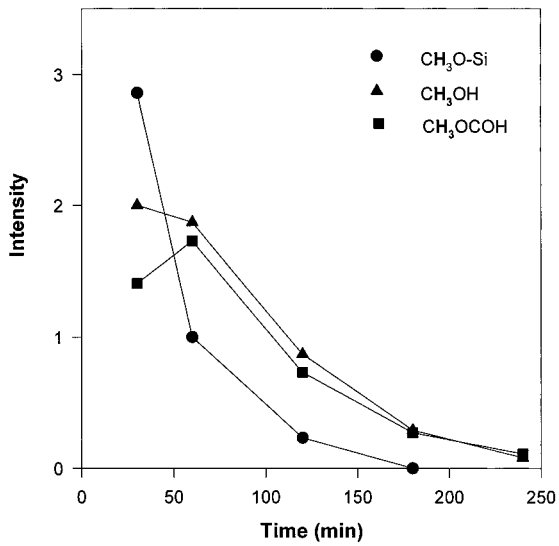

Figure 5. Evolution of the concentration of CH_3 protons pertaining to $Si(OCH_3)$ groups, CH_3OH and $HCOOCH_3$, during the first 4 h of reaction at 70 °C (synthesis of SSO3). The intensity gives the number of protons per 1 mol of 3-(methacryloxy)propyl groups.

discussed later. Their concentration was extremely small when compared with the concentration of residual SiOH groups.

SEC Characterization of SSOs at Advanced Degrees of Condensation. SEC chromatograms for the SSOs synthesized under different conditions are shown in Figure 7. Average molar masses for peaks 1−3, based on polystyrene standards, are indicated in Table 2.

The six SSOs may be ordered in three different pairs according to their relative degrees of condensation. SSO1 and SSO2 were the less condensed and exhibited similar molar mass distributions. However, the addition of water to the initial formulation produced a significant decrease of the polycondensation rate. Similar advances in the reaction were observed after 2 days of reaction at 50 °C when using concentrated formic acid or 12 days when adding extra water to the initial formulation. This may be ascribed to different reasons: (a) dilution effect,

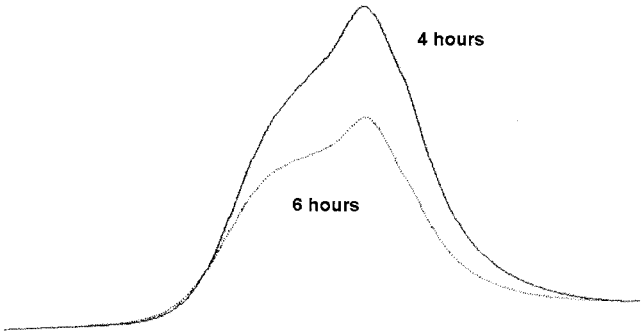

Figure 6. SEC chromatograms of the product distribution at about the end of the first stage of the synthesis (precursor of SSO3 after 4 and 6 h at 70 °C).

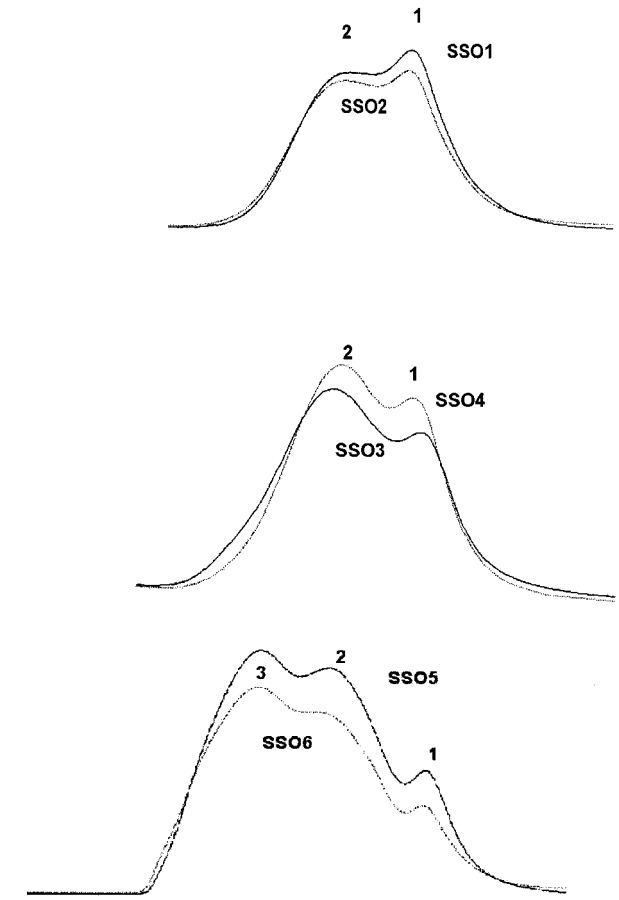

Figure 7. SEC chromatograms for the SSOs synthesized under different conditions. Average molar masses for peaks 1−3, based on PS standards, are shown in Table 2.

Table 2. Average Molar Masses (Da) of SEC Peaks (1−3), Based on PS Standards

	1			2			3		
notation	% area	M_n	M_w	% area	M_n	M_w	% area	M_n	M_w
SSO1	52	1130	1312	48	3200	3581			
SSO2	46	1132	1295	54	3163	3603			
SSO3	29	1205	1318	71	3702	4828			
SSO4	35	1241	1361	65	3472	4188			
SSO5	14	1178	1351	36	3686	4089	50	15 510	25 662
SSO6	12	1188	1360	34	3743	4151	54	16 232	28 891

(b) change in the polarity of the reaction medium, (c) fast conversion of $Si(OCH_3)$ groups to Si−OH groups, followed by a slow condensation reaction of these groups (the possibility of producing the condensation through eq 2 is lost).

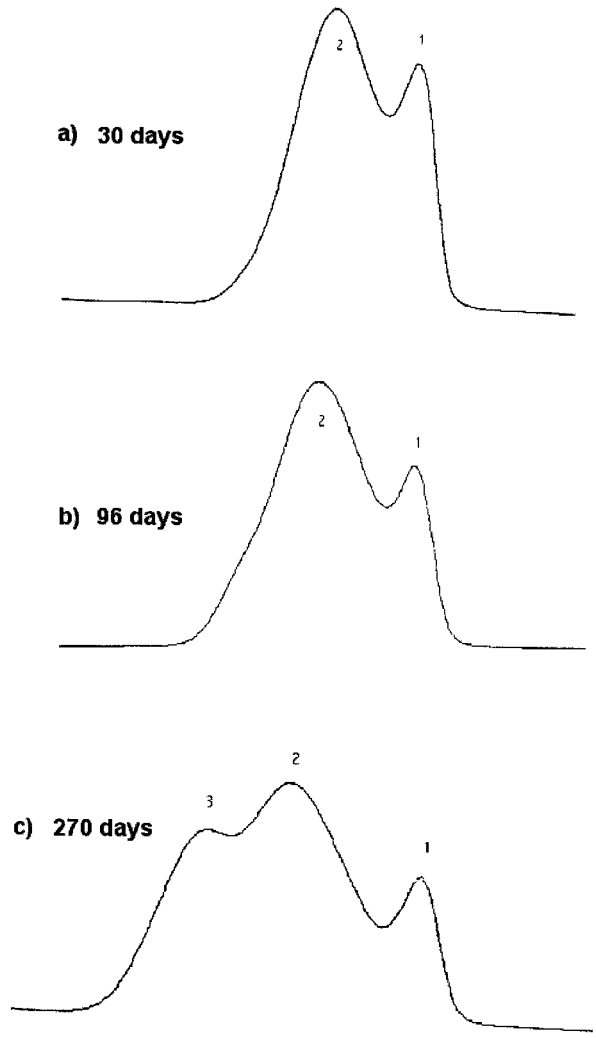

Figure 8. Evolution of SEC chromatograms of SSO2, after storage during different periods at 23 °C: (a) after 30 days; (b) after 96 days; (c) after 270 days.

SSO3 and SSO4 exhibited an intermediate degree of condensation as reflected by the increase in the area of the second peak at the expense of the first one. Molar mass distributions were similar, indicating that doubling the formic acid amount in the formulation had no significant effect on the condensation rate. The more condensed products, SSO5 and SSO6, exhibited similar molar mass distributions characterized by the presence of three peaks in SEC chromatograms.

The low-molar-mass peak in SEC chromatograms decreased its intensity with the advance in the condensation reaction but kept a constant location in the molar mass range. The average molar masses corresponded to species with 7−8 Si atoms on the basis of PS standards. The second peak in SEC chromatograms exhibited an initial increase in intensity at the expense of the first peak but a subsequent decrease in intensity as the third peak appeared. Average molar masses lead to species with about 18−20 Si atoms. The third chromatographic peak included high-molar-mass species containing about 50−200 Si atoms/molecule. The synthesis of SSOs exhibiting multimodal distribution of molar masses has been previously reported in the literature.[8,18]

The evolution of the molar mass distribution of SSO2 during storage at 23 °C was followed by SEC (Figure 8). In the absence of formic acid, the polycondensation

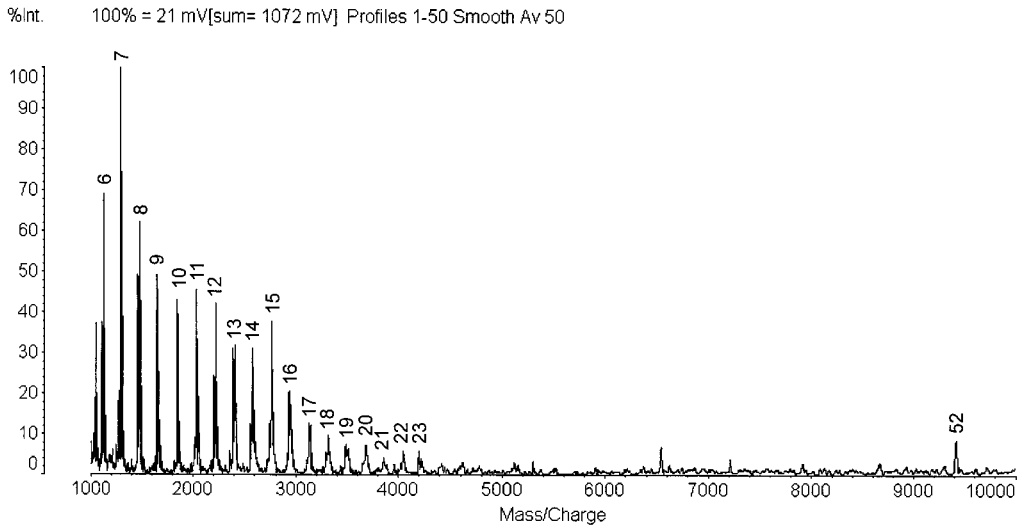

Figure 9. UV−MALDI−TOF MS of SSO1 using IAA as the matrix (instrument: MALDI III, positive-ion, linear mode).

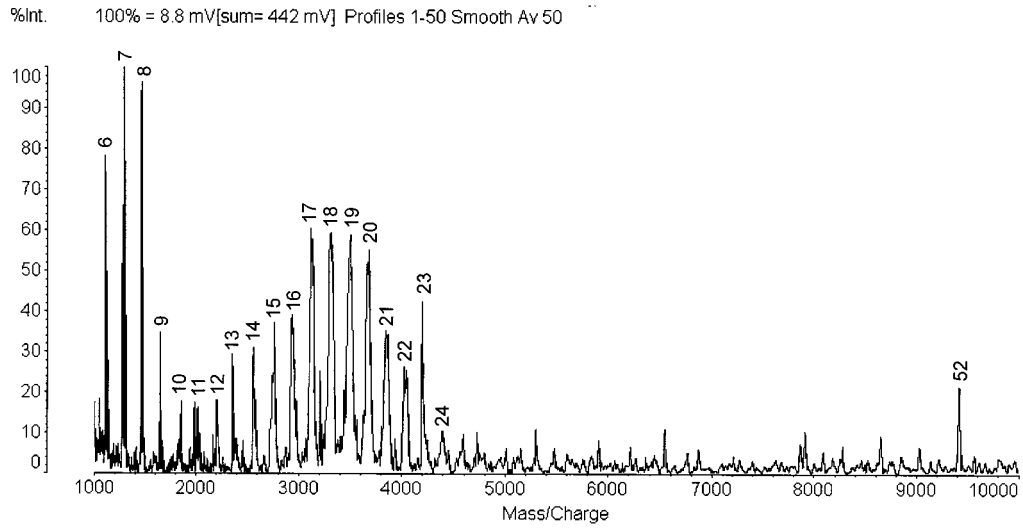

Figure 10. UV−MALDI−TOF MS of SSO2 using GA as the matrix (instrument: MALDI III, positive-ion, linear mode).

reaction between SiOH groups proceeded at a very slow rate. The second peak increased in intensity, and the third peak appeared after prolonged periods of storage.

The same main reaction pathway leading to three characteristic peaks in SEC chromatograms took place under different reaction conditions. This is visualized as follows. During the first stage of the reaction, species containing 6−8 Si atoms were formed through inter- and intramolecular condensation reactions. In parallel with this process, the more open species present in the cluster with 6−8 Si atoms reacted among themselves and with their reaction products, giving the distribution of species present in the second cluster (second peak of the SEC chromatogram). As the more open species disappeared from the first peak, the remaining species were those with larger fractions of intramolecular cycles (polyhedra and incompletely condensed polyhedra) that became less and less reactive. This explains the persistence of the first peak of the SEC chromatogram in highly condensed products. The slow intermolecular condensation of species present in the second cluster gave the third peak of the chromatogram.

UV−MALDI−TOF MS Characterization of SSOs at Advanced Degrees of Condensation. Figures 9−11 show UV−MALDI−TOF mass spectra of SSO1 (with IAA as the matrix), SSO2 (with GA as the matrix), and SSO4 (with GA as the matrix) in the positive-ion, linear mode. The number of Si atoms of the most significant species are indicated in each of the spectra.

For both SSO2 and SSO4, the presence of a bimodal distribution of molar masses is in qualitative agreement with the distributions shown in SEC chromatograms (Figure 7). For SSO1, the presence of a bimodal distribution was not so evident in the mass spectra. We found that small variations in the irradiation power or in the analyte/matrix ratio caused variations in the shape of the molar mass distribution curve. Although MALDI MS results could not replace SEC chromatograms to assess molar mass distributions, they were still useful to determine the mass, and the corresponding fraction of intramolecular cycles, of species present in significant concentrations.

For the spectra showing bimodal distributions, species with 7 and 8 Si atoms were present in significant concentrations in the first peak while species with 17−20 Si atoms were among the most significant of the second peak, in agreement with assignments made on SEC chromatograms based on PS standards.

Accurate assignments of (mass/charge) values to the UV−MALDI−TOF MS peaks were achieved when op-

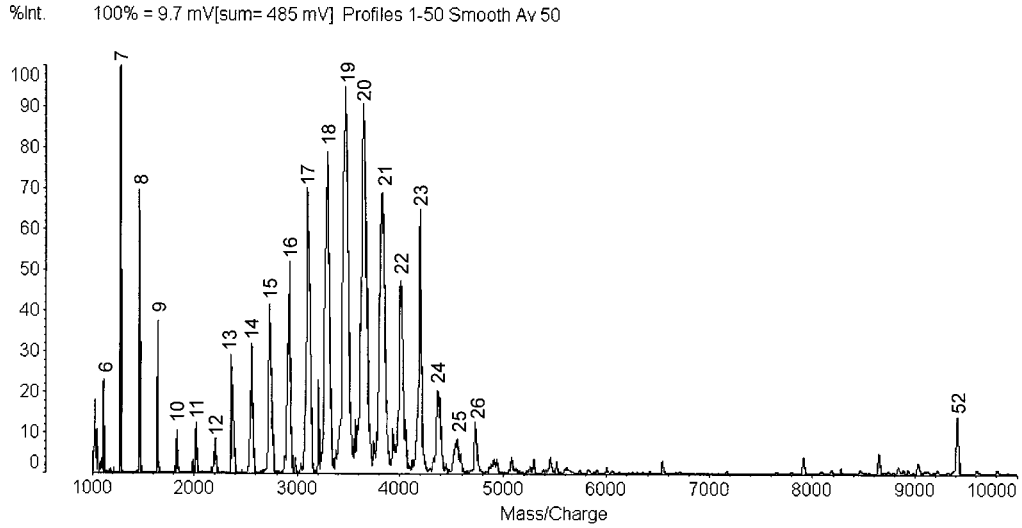

Figure 11. UV−MALDI−TOF MS of SSO4 using GA as the matrix (instrument: MALDI III, positive-ion, linear mode).

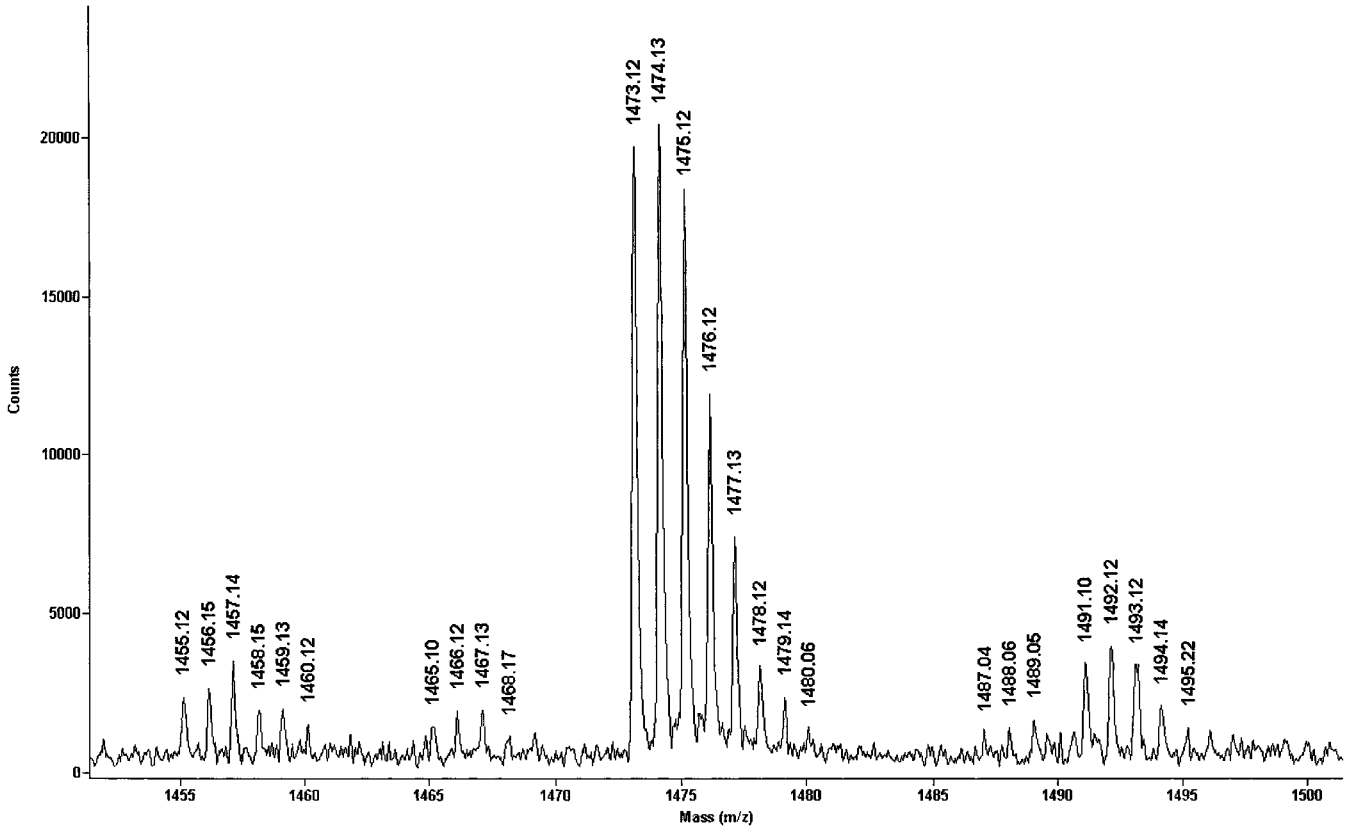

Figure 12. UV−MALDI−TOF MS of SSO2 (*m*/*z* range = 1450−1510 Da) in the reflector positive-ion mode (instrument: Voyager-DE-STR, GA as the matrix).

erating in the reflector mode. Ion reflection filters out neutral molecules, corrects time dispersion due to initial kinetic energy distribution, and provides greater mass accuracy. As an example, Figure 12 shows an UV−MALDI−TOF MS for SSO2, obtained in the reflector mode, in the *m*/*z* range between 1450 and 1510 Da. The most intense cluster of peaks was assigned to a $T_8(OH)_2$ species, ionized with Na^+ (theoretical value for the average isotopic composition = 1475.0 Da). The presence of several peaks around the average theoretical value is due to the isotopic distribution. No clusters corresponding to the ionization with H^+ (principal peaks expected at 1451.0, 1452.0, and 1453.0 Da), or with K^+ (principal peaks expected at 1489.1, 1490.1, and 1491.1 Da), were present. Besides, the (almost) exact agreement between theoretical and experimental masses proved that the organic residue [3-(methacryloxy)propyl] was kept intact in the course of the polycondensation process.

The cluster between 1491.1 and 1495.2 Da was assigned to $T_8(OH)_4$ ionized with Na^+ (theoretical value for the average isotopic composition = 1493.0 Da). The cluster between 1455.1 and 1460.1 Da was assigned to T_8 ionized with Na^+ (theoretical value for the average isotopic composition = 1457.0 Da). Therefore, for a given value of *n* Si atoms, a distribution of species with different *m* values (number of residual OH groups) appeared in the mass spectra. For SSO2 and *n* = 8, the

Table 3. Assignment of Peaks of UV−MALDI−TOF Mass Spectra of SSO1, SSO2, and SSO4 (*m/z*, Da) and Fraction of Intramolecular Cycles (*f*; Experimental and Predicted Values Corresponding to Ionization with Na^+)

	SSO1			SSO2			SSO4		
n	*m/z* (exp)	species (*m/z*)	*f*	*m/z* (exp)	species (*m/z*)	*f*	*m/z* (exp)	species (*m/z*)	*f*
6	1133	$T_6(OH)_4$ (1134)	0.50	1115	$T_6(OH)_2$ (1116)	0.75	1116	$T_6(OH)_2$ (1116)	0.75
7	1302	$T_7(OH)_3$ (1305)	0.75	1303	$T_7(OH)_3$ (1305)	0.75	1284	$T_7(OH)$ (1287)	1
8	1490	$T_8(OH)_4$ (1493)	0.60	1473	$T_8(OH)_2$ (1475)	0.80	1472	$T_8(OH)_2$ (1475)	0.80
9	1661	$T_9(OH)_3$ (1663)	0.80	1643	$T_9(OH)$(1645)	1	1643	$T_9(OH)$ (1645)	1
10	1849	$T_{10}(OH)_4$ (1851)	0.67	1851	$T_{10}(OH)_4$(1851)	0.67	1832	$T_{10}(OH)_2$ (1833)	0.83
11	2036	$T_{11}(OH)_5$ (2040)	0.67	2019	$T_{11}(OH)_3$ (2022)	0.83	2021	$T_{11}(OH)_3$ (2022)	0.83
12	2224	$T_{12}(OH)_6$ (2228)	0.57	2208	$T_{12}(OH)_4$ (2210)	0.71	2209	$T_{12}(OH)_4$ (2210)	0.71
13	2414	$T_{13}(OH)_7$ (2416)	0.57	2364	$T_{13}(OH)$ (2362)	1	2363	$T_{13}(OH)$ (2362)	1
14	2582	$T_{14}(OH)_6$ (2586)	0.62	2568	$T_{14}(OH)_4$ (2568)	0.75	2568	$T_{14}(OH)_4$ (2568)	0.75
15	2771	$T_{15}(OH)_7$ (2775)	0.62	2775	$T_{15}(OH)_7$ (2775)	0.62	2743	$T_{15}(OH)_3$ (2739)	0.87
16	2941	$T_{16}(OH)_6$ (2945)	0.67	2937	$T_{16}(OH)_6$ (2945)	0.67	2930	$T_{16}(OH)_4$ (2927)	0.78
17	3130	$T_{17}(OH)_7$ (3133)	0.67	3111	$T_{17}(OH)_5$ (3115)	0.78	3094	$T_{17}(OH)_3$ (3097)	0.89
18	3314	$T_{18}(OH)_8$ (3321)	0.60	3300	$T_{18}(OH)_6$ (3303)	0.70	3303	$T_{18}(OH)_6$ (3303)	0.70
19	3490	$T_{19}(OH)_7$ (3492)	0.70	3497	$T_{19}(OH)_7$ (3492)	0.70	3487	$T_{19}(OH)_7$ (3492)	0.70
20	3695	$T_{20}(OH)_{10}$ (3698)	0.55	3694	$T_{20}(OH)_{10}$ (3698)	0.55	3655	$T_{20}(OH)_6$ (3662)	0.73
21	3861	$T_{21}(OH)_9$ (3868)	0.64	3844	$T_{21}(OH)_7$ (3850)	0.73	3844	$T_{21}(OH)_7$ (3850)	0.73
22	4057	$T_{22}(OH)_{10}$ (4056)	0.58	4027	$T_{22}(OH)_6$ (4020)	0.75	4009	$T_{22}(OH)_4$ (4002)	0.83
23	4196	$T_{23}(OH)_5$ (4191)	0.83	4195	$T_{23}(OH)_5$ (4191)	0.83	4186	$T_{23}(OH)_5$ (4191)	0.83
24	4414	$T_{24}(OH)_{10}$ (4415)	0.62	4387	$T_{24}(OH)_6$ (4379)	0.77	4397	$T_{24}(OH)_8$ (4397)	0.69
52	9419	$T_{52}(OH)_8$(9416)	0.85	9419	$T_{52}(OH)_8$ (9416)	0.85	9420	$T_{52}(OH)_8$ (9416)	0.85

most significant species was the one with $m = 2$ (incompletely condensed polyhedron with a fraction of intramolecular cycles, $f = 0.8$; Figure 1).

There were still two other clusters of very low intensity present in Figure 12. The one between 1465.1 and 1468.2 Da was assigned to $T_{16}(OH)_2$, ionized with 2 Na^+ ions (*m/z* values correspond to $z = 2$). The theoretical value for the average isotopic composition is 1466.0 Da, in excellent agreement. The cluster comprising peaks at 1487−1489 Da, which was barely discernible, was assigned to $T_8(OH)(OCH_3)$ ionized with Na^+ (theoretical value for the average isotopic composition = 1489.0 Da). It may be concluded that traces of $Si(OCH_3)$ groups were still present in SSO2.

On the basis of the accurate assignment of peaks present in the mass spectrum obtained in the reflector mode, the assignment of main peaks of mass spectra obtained in the linear mode (Figures 9−11) was carried out by assuming that *m/z* values corresponded to $T_n(OH)_m$ species ionized with Na^+. Another proof of the fact that recorded species were ionized with Na^+ was obtained by doping the samples with NaCl and observing the same spectra without any significant shift. Doping with AgTFA generated a subset of less intense peaks shifted by 85 Da, the difference between the atomic masses of Ag^+ and Na^+.

Table 3 shows the assignment of the main peaks present in the mass spectra of Figures 9−11. Species containing 6−24 Si atoms are indicated, together with a species with 52 Si atoms, $T_{52}(OH)_8$. This species, which appeared in relatively significant concentrations in every one of the SSOs, must exhibit a particularly stable structure.

The agreement between experimental values and theoretical assignments may be considered reasonable, taking into account that (a) operating in the linear mode produces a time dispersion, and consequently a dispersion in recorded masses, due to the initial kinetic energy distribution of ions that adds to the isotopic distribution, (b) the overlapping of peaks corresponding to species with different *m* values, for intermediate and high *n* values, produces maxima that may be shifted with respect to the theoretical values, particularly for low-intensity peaks.

The three SSOs exhibited the presence of species containing a high fraction of intramolecular cycles, $f = 0.5-1$. For *n* values between 6 and 24, the average value of intramolecular cycles was $f_{av} = 0.64$ for SSO1, $f_{av} = 0.76$ for SSO2, and $f_{av} = 0.81$ for SSO4. Although SSO1 and SSO2 showed similar molar mass distributions in SEC chromatograms (Figure 7), the former contained species with more open structures than the latter. This would account for the need to select different matrixes for both SSOs in MALDI−TOF MS experiments to obtain peaks with enough intensity in the *m/z* range of interest.

An explanation of the different fractions of intramolecular cycles in SSO1 and SSO2 may be postulated on the basis of recent results reported by Matejka et al.[7] For SSOs synthesized under basic or neutral conditions with an H_2O/Si ratio equal to 1.5, they found evidence of an organized structure of regularly arranged domains of compact cagelike frameworks, as resulted from the sharp interference maxima in SAXS (small-angle X-ray scattering) intensity profiles. They attributed this microphase separation to the incompatibility of the SSO network and pendant organic chains. Under conditions of phase separation, intramolecular condensation reactions should be enhanced. The situation was quite different when acid catalysts were used, keeping the same ratio of H_2O/Si. This produced less polyhedral structures and no regular arrangement. The invoked reason was a fast initial hydrolysis leading to a high content of SiOH groups. The increased H-bond interactions of these groups with oxygen atoms in the organic chains led to a better compatibility, restricting the possibility of phase separation. Under these conditions, intermolecular reactions should be significant, leading to the formation of more open structures. The same explanation may be used in our case. When using 98 wt % formic acid to produce the polycondensation, as is the case of SSO2, the reaction between Si−OOCH groups and $Si-OCH_3$ groups (eq 2) may lead to a high fraction of intramolecular cycles in segregated SSO domains. The fast hydrolysis produced during the synthesis of SSO1 leads to a high fraction of SiOH groups H-bonded to carbonyl groups of the organic residues. This should prevent microphase separation,

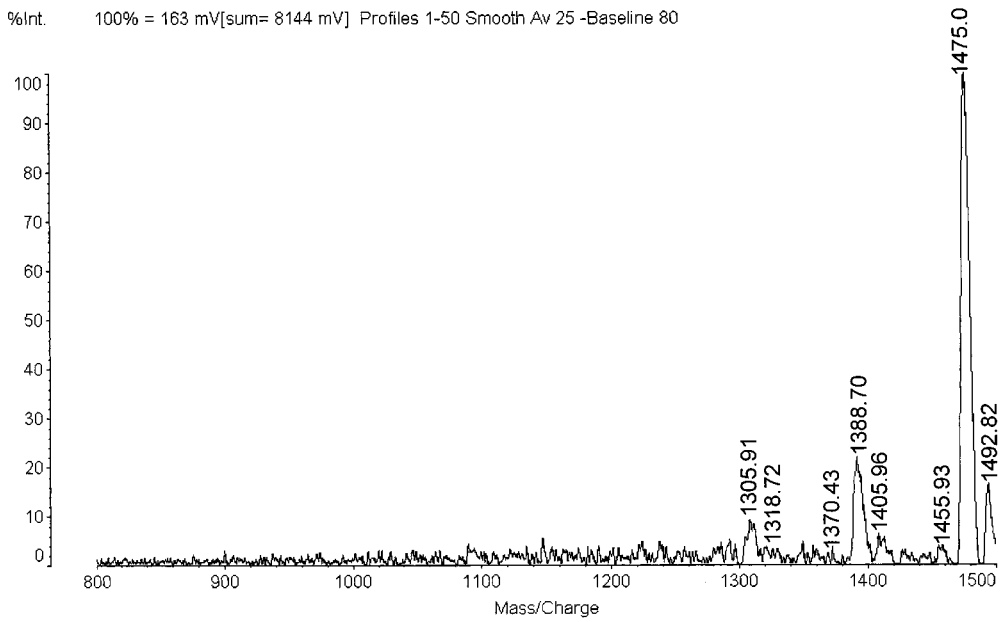

Figure 13. UV−MALDI−TOF MS of SSO2 (m/z range = 800−1500 Da) in the PSD mode. Gate: m/z range = 1405−1559 Da (instrument: MALDI 4, positive-ion mode, GA as the matrix).

increasing the probability of producing intermolecular condensation reactions.

As the degree of polycondensation increases, e.g., comparing SSO2 and SSO4, the average fraction of intramolecular cycles is also increased. Polyhedra and incompletely condensed polyhedra are found in significant concentrations in the distribution of reaction products.

MS/MS analysis of selected precursors was also performed. Metastable fragmentation in the field-free region, called PSD, was observed in the reflector mode. Figure 13 shows an example for SSO2 and a gate (m/z = 1405−1559 Da), corresponding to the precursor $T_8(OH)_2$ ionized with Na^+ (theoretical mass = 1475.0 Da). The selected gate included species at 1492.8 and 1455.9 Da ascribed to $T_8(OH)_4$ (theoretical mass with Na^+ equal to 1493.0 Da) and T_8 (theoretical mass with Na^+ equal to 1457.0 Da). The fragmentation pattern was quite simple in agreement with the cagelike structures of the selected precursor. The three fragment ions at 1370.4, 1388.7, and 1406.0 Da involved the loss of about 86 Da from the precursors. A second subset of peaks corresponding to species that have lost about twice this mass also appeared in the mass spectrum with a smaller intensity. A similar phenomenon was observed when selecting other ions as precursors. The ejected fragment with a mass close to 86 Da was a neutral species (it was not detected as an ionized fragment) and may be assigned to methacrylic acid. Therefore, fragmentation in the PSD mode occurred at one or more of the organic groups joined to Si atoms, through the following reaction:

$$[-Si-CH_2-CH_2-CH_2-O-CO-C(CH_3)=CH_2]^+ \rightarrow [-Si-CH_2-CH=CH_2]^+ + HO-CO-C(CH_3)=CH_2$$

This constitutes a characteristic decomposition of esters called "rearrangement of one hydrogen atom or McLafferty rearrangement".[19]

ESI−TOF MS Characterization of SSOs at Advanced Degrees of Condensation. ESI−TOF mass spectra of SSO1 and SSO2 are respectively shown in Figures 14 and 15. The assignment of main peaks is indicated in Tables 4 and 5. An excellent agreement between experimental and predicted values could be obtained by assuming that species were charged with one or two Na^+ cations. Species containing (OCH_3) groups that were present as traces in UV−MALDI−TOF mass spectra were observed with relatively higher intensities in ESI−TOF mass spectra. The distribution of intensities in these spectra is governed by the facility with which species are ionized and should not be used to estimate the absolute concentrations of different species. However, ESI−TOF mass spectra were indeed useful to follow the evolution of particular species during the polycondensation.

When the species present in SSO1 and SSO2 were compared, it was again found that the former exhibited the presence of more open structures than the latter. For example, species $T_7(OH)$ (f = 1) and $T_9(OH)$ (f = 1) could only be detected in SSO2 in the defined range of relative intensities; species $T_4(OH)_4$ (f = 0.33) and $T_{10}(OH)_6$ (f = 0.50) could only be detected in SSO1, in a similar range of relative intensities.

Table 4. Assignment of the Main Peaks Present in the ESI−TOF Mass Spectra of SSO1

intensity	z	assignment	exptl m/z (Da)	calcd $(M + zNa^+)/z$ (Da)
100	2	$T_8(OH)_2$	748.7	749.0
50−60	1	$T_7(OH)_3$	1304.3	1304.7
	2	$T_9(OH)_3$	843.2	843.1
40−50	1	$T_4(OH)_4$	775.2	776.0
	1, 2	$T_6(OH)_2$, $T_{12}(OH)_4$	1116.3	1116.5
	1	$T_6(OH)_4$	1133.3	1134.5
	1	$T_8(OH)_2$	1474.4	1475.0
	2	$T_{10}(OH)_4$	937.2	937.2
30−40	2	$T_7(OH)_3$	663.2	663.8
	2	$T_8(OH)_4$	757.2	758.0
20−30	1	$T_6(OH)_3(OCH_3)$	1147.3	1148.5
	1	$T_7(OH)_2(OCH_3)$	1318.4	1318.7
	2	$T_7(OH)_2(OCH_3)$	670.2	670.8
	2	$T_{10}(OH)_2$	927.2	928.2
	2	$T_{10}(OH)_6$	946.2	946.2
	2	$T_{11}(OH)_3$	1022.3	1022.3
	2	$T_{11}(OH)_5$	1031.3	1031.3

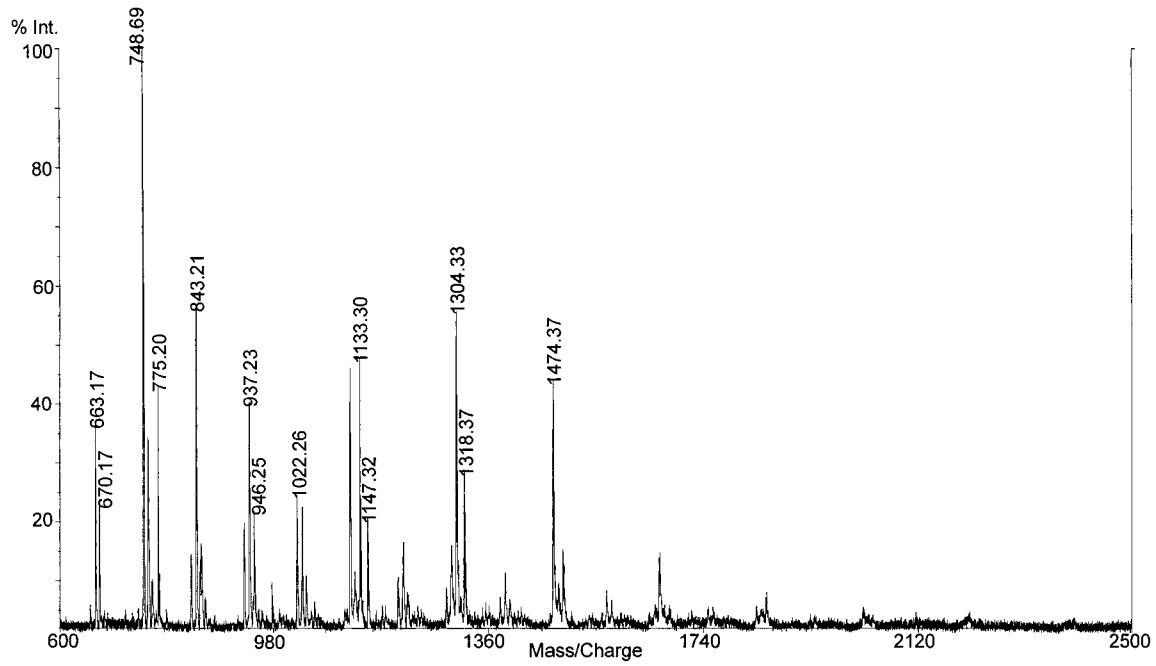

Figure 14. ESI−TOF MS of SSO1 (positive-ion mode).

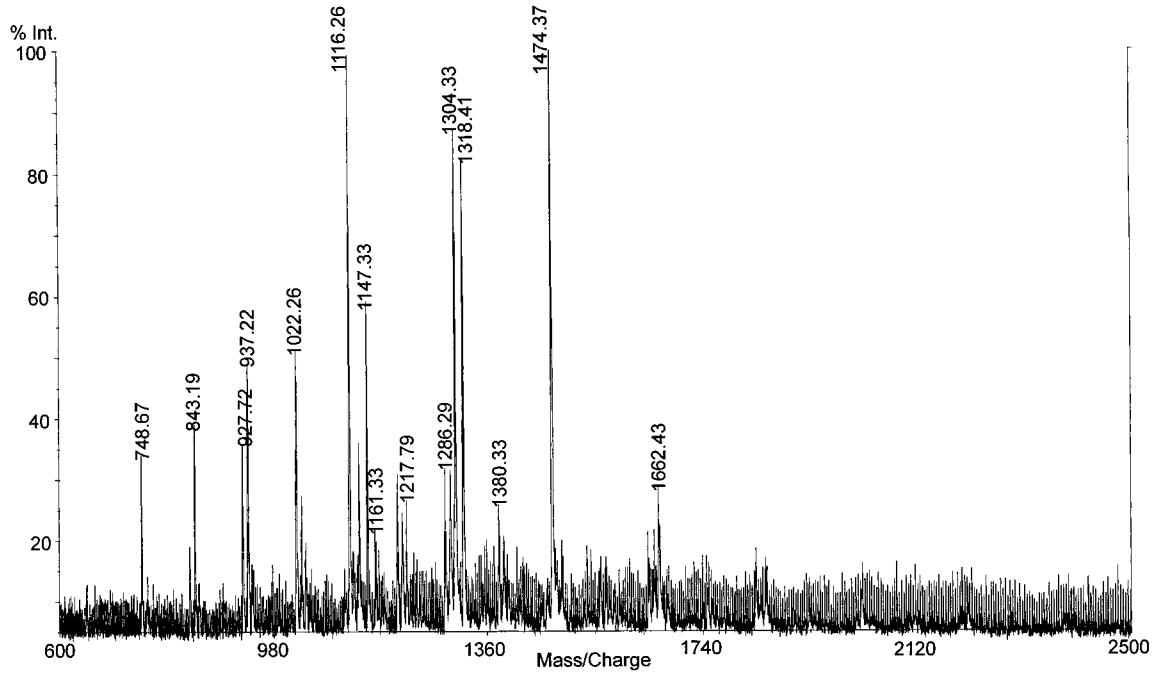

Figure 15. ESI−TOF MS of SSO2 (positive-ion mode).

The fate of these species could be followed by comparing ESI−TOF mass spectra of SSO2 and SSO3 (the temperature variation is assumed to affect the reaction rate but not the reaction path). ESI−TOF MS of SSO3 is shown in Figure 16. Again, the assignment of peaks could be made by assuming that every species incorporated one or two Na^+ cations. Table 6 presents a comparison of the main species present in both SSOs in three ranges of relative intensities. $T_8(OH)_2$ was the most significant species of those remaining in the first peak of the SEC chromatogram at more advanced conversions. This gives a hint of its particular stability toward condensation reactions. A significant decrease in the intensity of species containing (OCH_3) groups was also observed. This may be caused either by their participation in condensation reactions or by the hydrolysis of the methoxy group produced by H_2O originating in SiOH + SiOH condensation reactions. In general, the more open species have disappeared or decreased their intensities at higher conversions in the polycondensation reaction. This is the case of $T_6(OH)_4$, $T_6(OH)_3(OCH_3)$, $T_6(OH)_2(OCH_3)_2$, $T_{11}(OH)_5$, $T_{11}(OH)_4(OCH_3)$, etc. Therefore, residual species in the first peak of the SEC chromatogram are those exhibiting a higher fraction of intramolecular cycles. These species are less reactive in condensation reactions possibly because of steric hindrance effects. The same process is plausibly operative for the whole population of species: "open" species are condensed at a faster rate than "closed" species both by inter- and intramolecular reactions,

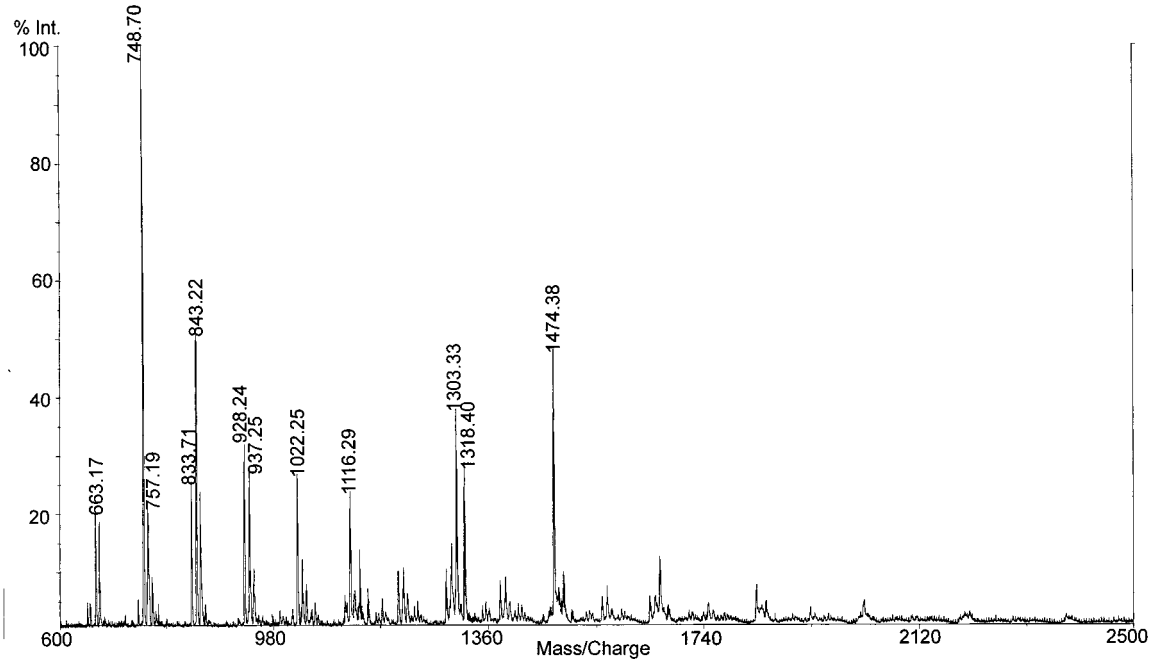

Figure 16. ESI−TOF MS of SSO3 (positive-ion mode).

Table 5. Assignment of the Main Peaks Present in the ESI−TOF Mass Spectra of SSO2

intensity	*z*	assignment	exptl *m/z* (Da)	calcd $(M + zNa^+)/z$ (Da)
80−100	1, 2	$T_6(OH)_2$, $T_{12}(OH)_4$	1116.3	1116.5
	1	$T_7(OH)_3$	1304.3	1304.7
	1	$T_7(OH)_2(OCH_3)$	1318.4	1318.7
	1	$T_8(OH)_2$	1474.4	1475.0
50−60	1	$T_6(OH)_3(OCH_3)$	1147.3	1148.5
	2	$T_{11}(OH)_3$	1022.3	1022.3
40−50	2	$T_{10}(OH)_4$	937.2	937.2
30−40	1	$T_6(OH)_4$	1133.3	1134.5
	1, 2	$T_7(OH)$, $T_{14}(OH)_2$	1286.3	1286.7
	2	$T_8(OH)_2$	748.7	749.0
	2	$T_9(OH)_3$	843.2	843.1
	2	$T_{10}(OH)_2$	927.7	928.2
	2	$T_{13}(OH)_3$	1200.8	1201.6
	2	$T_{14}(OH)_4$	1295.0	1295.7
20−30	1	$T_6(OH)_2(OCH_3)_2$	1161.3	1162.5
	1	$T_9(OH)$	1644.0	1645.2
	1	$T_9(OH)_3$	1662.4	1663.2
	2	$T_{11}(OH)_5$	1031.7	1031.3
	2	$T_{13}(OH)_5$	1210.3	1210.6
	2	$T_{13}(OH)_4(OCH_3)$	1217.8	1217.6
	2	$T_{15}(OH)_3$	1380.3	1380.8
	2	$T_{18}(OH)_4$	1654.0	1654.2

implying that the fraction of intramolecular cycles should increase continuously with conversion.

The sequence SSO4 and SSO6 may also be used to analyze the evolution of main species during the polycondensation in the second stage. ESI−TOF mass spectra of these products are shown in Figures 17 and 18. As with the other SSOs, a precise assignment of peaks could be made by assuming that every species incorporated one or two Na^+ cations. Results are shown in Table 7.

The comparison of species present in SSO4 and SSO6 (Table 7) clearly shows that, at advanced conversions, the residual species present in the first peak of the SEC chromatogram exhibit a very large fraction of intramolecular cycles. Most of them are perfect polyhedra, like T_8, or incompletely condensed polyhedra, like

Table 6. Main Species Present in the ESI−TOF Mass Spectra of SSO2 and SSO3

intensity	*z*	SSO2 assignment	*z*	SSO3 assignment
high (80−100)	1, 2	$T_6(OH)_2$, $T_{12}(OH)_4$	2	$T_8(OH)_2$
	1	$T_7(OH)_2(OCH_3)$		
	1	$T_7(OH)_3$		
	1	$T_8(OH)_2$		
medium (30−80)	1	$T_6(OH)_3(OCH_3)$	1	$T_7(OH)_3$
	1	$T_6(OH)_4$	1	$T_8(OH)_2$
	1, 2	$T_7(OH)$, $T_{14}(OH)_2$	2	$T_9(OH)_3$
	2	$T_8(OH)_2$	2	$T_{10}(OH)_2$
	2	$T_9(OH)_3$		
	2	$T_{10}(OH)_2$		
	2	$T_{10}(OH)_4$		
	2	$T_{11}(OH)_3$		
	2	$T_{13}(OH)_3$		
	2	$T_{14}(OH)_4$		
low (20−30)	1	$T_6(OH)_2(OCH_3)_2$	2	$T_7(OH)_3$
	1	$T_9(OH)$	1	$T_7(OH)_2(OCH_3)$
	1	$T_9(OH)_3$	2	$T_8(OH)_4$
	2	$T_{11}(OH)_5$	2	$T_9(OH)$
	2	$T_{13}(OH)_4(OCH_3)$	2	$T_9(OH)_2(OCH_3)$
	2	$T_{13}(OH)_5$	2	$T_{10}(OH)_4$
	2	$T_{15}(OH)_3$	2	$T_{11}(OH)_3$
	2	$T_{18}(OH)_4$	2	$T_{12}(OH)_4$

$T_8(OH)_2$, $T_9(OH)$, or $T_{10}(OH)_2$. The more "open" species have disappeared from the distribution in the considered intensity range. This evidences that the average fraction of intramolecular cycles increases continuously along the polymerization.

Conclusions

The polycondensation of MPMS in bulk, using 98 wt % formic acid, was followed with a set of experimental techniques: ^1H NMR, FTIR, SEC, UV−MALDI−TOF MS (linear, reflector, and PSD modes), and ESI−TOF MS. The first stage of the process was characterized by the rapid generation of methanol and methyl formate. This was ascribed to the formation of Si−OOCH groups with elimination of CH_3OH and the subsequent fast condensation reaction of Si−OOCH and Si−(OCH_3) groups, generating the ester as the byproduct. The main structures produced through these reactions contained

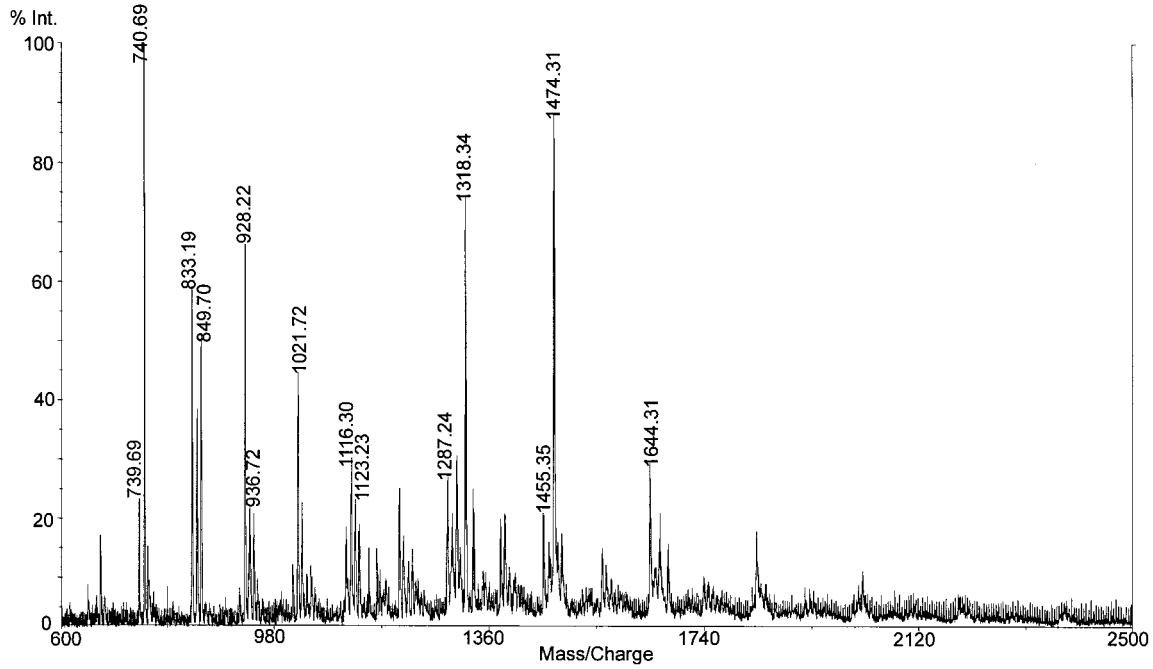

Figure 17. ESI−TOF MS of SSO4 (positive-ion mode).

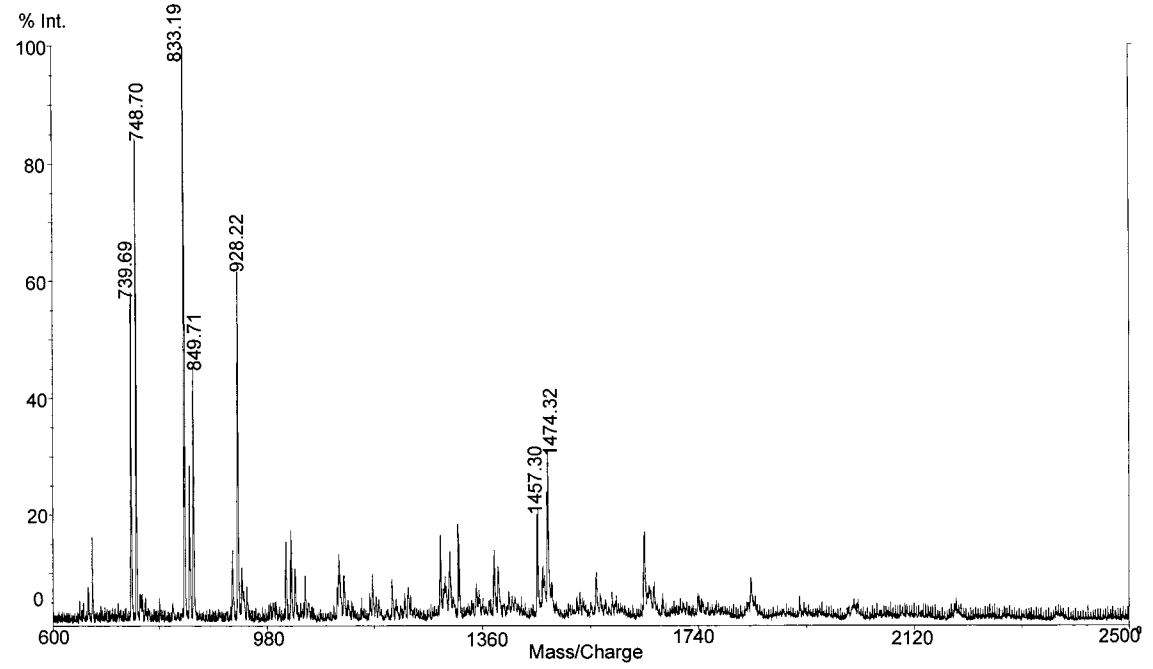

Figure 18. ESI−TOF MS of SSO6 (positive-ion mode).

a very large fraction of intramolecular cycles. The ester was continuously removed from the reaction medium, particularly when performing the synthesis at 70 °C. After 2 days of reaction at 50 °C, or about 6 h at 70 °C, reactive positions of the resulting SSO were mainly Si−OH groups, with only traces of $Si-OCH_3$ groups. The residual amounts of species with $n = 1$ (monomer) up to $n = 4$ (tetramer) were practically negligible, indicating that the reactivity of any group in the condensation reaction decreased with an increase of the molar mass of the species to which it belonged. This was ascribed to negative substitution effects produced by Si−O−Si bonds joined to the same Si atom and/or to steric effects produced by the formation of intramolecular cycles that led to more compact structures. After this time, the polycondensation continued slowly during storage at room temperature, basically through Si−OH + Si−OH reactions. The average fraction of intramolecular cycles increased continuously during the polycondensation. An average value, $f_{av} = 0.81$, was found for species containing 6−24 Si atoms. In MS/MS spectra, these closed structures showed the fragmentation of one or more of the ester groups joined to Si atoms, by a McLafferty rearrangement. The addition of water to the initial formulation (about a 3:1 H_2O/Si molar ratio) led a slower polycondensation rate and to a decrease of the average fraction of intramolecular cycles (formation of more open structures). When using 98 wt % formic acid to produce

Table 7. Main Species Present in the ESI−TOF Mass Spectra of SSO4 and SSO6

intensity	*z*	SSO4 assignment	*z*	SSO6 assignment
high (80−100)	1	$T_8(OH)_2$	2	$T_8(OH)_2$
	2	$T_8(OH)_2$	2	$T_9(OH)$
medium (30−80)	1	$T_7(OH)_2(OCH_3)$	2	T_8
	2	$T_9(OH)$	1	$T_8(OH)_2$
	2	$T_9(OH)_2(OCH_3)$	2	$T_9(OH)_2(OCH_3)$
	2	$T_9(OH)_3$	2	$T_{10}(OH)_2$
	2	$T_{10}(OH)_2$		
	2		2	$T_{11}(OH)_3$
low (20−30)	1, 2	$T_7(OH)$, $T_{14}(OH)_2$	1	$T_7(OH)$
	1	$T_7(OH)_3$	1	$T_7(OH)_2(OCH_3)$
	1	$T_7(OH)(OCH_3)_2$	2	$T_7(OH)_2(OCH_3)$
	1	T_8	1	T_8
	1	$T_9(OH)$	1	$T_9(OH)$
	1	$T_9(OH)_3$	2	$T_9(OH)_3$
	2	$T_9(OH)_3$	2	$T_{11}(OH)$
	2	$T_{10}(OH)_4$	2	$T_{11}(OH)_3$
	2	$T_{10}(OH)_3(OCH_3)$	2	$T_{12}(OH)_2$
	2	$T_{11}(OH)_2(OCH_3)$		
	2	$T_{12}(OH)_4$		
	2	$T_{12}(OH)_3(OCH_3)$		
	2	$T_{13}(OH)_3$		
	2	$T_{14}(OH)_4$		
	2	$T_{15}(OH)_3$		

the polycondensation, the reaction between Si−OOCH and $Si-OCH_3$ groups may lead to a high fraction of intramolecular cycles in segregated SSO domains. When water is added to the initial formulation, the fast hydrolysis gives a high fraction of SiOH groups H-bonded to carbonyl groups of the organic residues. This should prevent microphase separation, increasing the probability of producing intermolecular condensation reactions.

Acknowledgment. We acknowledge the financial support of CONICET, ANPCyT, Universities of Buenos Aires and Mar del Plata, and INTI, Argentina. We thank Y. Fukuyama for the experiments in a Voyager DE-STR spectrometer. Mass spectrometry was performed as part of the Academic Agreement between R.E.-B. and H.N. with the facilities of the High Resolution Liquid Chromatography-integrated Mass Spectrometer System Laboratory of the United Graduate School of Agricultural Sciences (Ehime University, Japan).

References and Notes

(1) Baney, R. H.; Itoh, M.; Sakakibara, A.; Suzuki, T. *Chem. Rev.* **1995**, *95*, 1409.
(2) Sharp, K. *J. Sol−Gel Sci. Technol.* **1994**, *2*, 35.
(3) Wallace, W. E.; Guttman, C. M.; Antonucci, J. M. *J. Am. Soc. Mass Spectrom.* **1999**, *10*, 224.
(4) Wallace, W. E.; Guttman, C. M.; Antonucci, J. M. *Polymer* **2000**, *41*, 2219.
(5) Fasce, D. P.; Williams, R. J. J.; Méchin, F.; Pascault, J. P.; Llauro, M. F.; Pétiaud, R. *Macromolecules* **1999**, *32*, 4757.
(6) Fasce, D. P.; Williams, R. J. J.; Erra-Balsells, R.; Ishikawa, Y.; Nonami, H. *Macromolecules* **2001**, *34*, 3534.
(7) Matejka, L.; Dukh, O.; Hlavatá, D.; Meissner, B.; Brus, J. *Macromolecules* **2001**, *34*, 6904.
(8) Eisenberg, P.; Erra-Balsells, R.; Ishikawa, Y.; Lucas, J. C.; Mauri, A. N.; Nonami, H.; Riccardi, C. C.; Williams, R. J. J. *Macromolecules* **2000**, *33*, 1940.
(9) Nonami, H.; Wu, F.; Thummel, R. P.; Fukuyama, Y.; Yamaoka, H.; Erra-Balsells, R. *Rapid Commun. Mass Spectrom.* **2001**, *15*, in press.
(10) Brinker, C. J.; Assink, R. A. *J. Non-Cryst. Solids* **1989**, *111*, 48.
(11) Doughty, D. H.; Assink, R. A.; Kay, B. D. In *Silicon-Based Polymer Science*; Zeigler, J. M., Gordon Fearon, F. W., Eds.; Advances in Chemistry Series 224; American Chemical Society: Washington, DC, 1990; p 241.
(12) Bailey, J. K.; Macosko, C. W.; Mecartney, M. L. *J. Non-Cryst. Solids* **1990**, *125*, 208.
(13) Rankin, S. E.; Kasehagen, L. J.; McCormick A. V.; Macosko, C. W. *Macromolecules* **2000**, *33*, 7639.
(14) Feher, F. J.; Newman, D. A.; Walzer, J. F. *J. Am. Chem. Soc.* **1989**, *111*, 1741.
(15) Feher, F. J.; Soulivong, D.; Eklund, A. G. *Chem. Commun.* **1998**, 399.
(16) Feher, F. J.; Soulivong, D.; Nguyen, F. *Chem. Commun.* **1998**, 1279.
(17) Feher, F. J.; Budzichowski, T. A.; Blanski, R. L.; Weller, K. J.; Ziller, J. W. *Organometallics* **1991**, *10*, 2526.
(18) Piana, K.; Schubert, U. *Chem. Mater.* **1994**, *6*, 1504.
(19) McLafferty, F. W.; Turecek, F. *Interpretation of Mass Spectra*, 4th ed.; University Science Books: Sausalito, CA, 1993; p 81.

MA011305G